Toxicology and Applied Pharmacology 450 (2022) 116154

Contents lists available at ScienceDirect

Toxicology and Applied Pharmacology

journal homepage: www.elsevier.com/locate/taap

Biological effects of inhaled crude oil vapor. II. Pulmonary effects

Jeffrey S. Fedan [a,*], Janet A. Thompson [a], Kristen A. Russ [a], Richard D. Dey [b], Jeffrey S. Reynolds [a], Michael L. Kashon [a], Mark C. Jackson [a], Walter McKinney [a]

[a] Health Effects Laboratory Division, National Institute for Occupational Safety and Health, Morgantown, WV 26505, United States of America
[b] Department of Pathology, Anatomy and Laboratory Medicine, West Virginia University Health Sciences Center, Morgantown, WV 26506, United States of America

ARTICLE INFO

Editor: Lawrence Lash

Keywords:
Crude oil vapor
Lung
Pulmonary function
Toxicity
Inhalation exposure
Animal model
Rat

ABSTRACT

Workers involved in oil exploration and production in the upstream petroleum industry are exposed to crude oil vapor (COV). COV levels in the proximity of workers during production tank gauging and opening of thief hatches can exceed regulatory standards, and several deaths have occurred after opening thief hatches. There is a paucity of information regarding the effects of COV inhalation in the lung. To address these knowledge gaps, the present hazard identification study was undertaken to investigate the effects of an acute, single inhalation exposure (6 h) or a 28 d sub-chronic exposure (6 h/d × 4 d/wk × 4 wks) to COV (300 ppm; Macondo well surrogate oil) on ventilatory and non-ventilatory functions of the lung in a rat model 1 and 28 d after acute exposure, and 1, 28 and 90 d following sub-chronic exposure. Basal airway resistance was increased 90 d post-sub-chronic exposure, but reactivity to methacholine (MCh) was unaffected. In the isolated, perfused trachea preparation the inhibitory effect of the airway epithelium on reactivity to MCh was increased at 90 d post-exposure. Efferent cholinergic nerve activity regulating airway smooth muscle was unaffected by COV exposure. Acute exposure did not affect basal airway epithelial ion transport, but 28 d after sub-chronic exposure alterations in active (Na^+ and Cl^-) and passive ion transport occurred. COV treatment did not affect lung vascular permeability. The findings indicate that acute and sub-chronic COV inhalation does not appreciably affect ventilatory properties of the rat, but transient changes in airway epithelium occur.

1. Introduction

This is the second paper in a series of seven tandem papers which focus on an investigation of the effects of inhaled crude oil vapor using an animal inhalation model (Walter et al., 2022) on the pulmonary, cardiovascular, immune and nervous systems, brain and kidneys (Sager et al., 2022; Krajnak et al., 2022; Sriram et al., 2022; Weatherly et al., 2022). The purpose of the overall investigation is introduced in Fedan (2022) and the results obtained from these investigations have been summarized (Investigative Team, 2022).

Workers in the upstream segment of the oil and gas extraction industry, which includes exploration, drilling, storage and transportation of crude oil to refineries, are at risk of inhalation exposure to crude oil vapor while conducting routine tasks in or around petroleum storage tanks, such as manual gauging, sample collection, flow back operations, and tank cleaning and maintenance (Esswein et al., 2014a, 2014b; King et al., 2015; Snawder et al., 2014; Retzer et al., 2015, 2018). The release of hydrocarbon vapors and volatile organic vapor plumes (> 100,000 ppm) after the opening of the thief hatches on petroleum storage tanks resulted in the deaths of nine workers who were engulfed in the fumes (Snawder et al., 2014; Jordan, 2015; Harrison et al., 2016; National Institute for Occupational Safety and Health/Occupational Safety and Health Administration, 2015; Centers for Disease Control and Prevention. National Institute for Occupational Safety and Health, 2020a, 2020b). Additional information about the health effects of crude oil in humans in and out of the workplace setting is provided in Fedan (2022).

Crude oil is a complex mixture of hydrocarbons of different molecular weights (see Walter et al., 2022; Ritchie et al., 2001). There is abundant information about the pulmonary toxicities of individual ingredients in crude oil during downstream petroleum processing or use (Agency for Toxic Substances and Disease Registry, 1995, 1999, 2007, 2016). On the other hand, the potential toxicity of vapors of crude oil itself in the lungs is undescribed. Therefore, the present hazard identification investigation was designed to examine whether ventilatory and

* Corresponding author at: Pathology and Physiology Research Branch, National Institute for Occupational Safety and Health, 1000 Frederick Lane, Morgantown, WV 26508, United States of America.
E-mail address: jsf2@cdc.gov (J.S. Fedan).

https://doi.org/10.1016/j.taap.2022.116154
Received 24 March 2022; Received in revised form 22 June 2022; Accepted 30 June 2022
Available online 5 July 2022

non-ventilatory functions of the lungs are affected by inhalation of crude oil vapor (COV) using a rat inhalation model.

2. Methods

2.1. Animals

All studies were conducted in facilities accredited by AAALAC International, were approved by the Institutional Animal Care and Use Committee (protocols 13-JF-R-014, 14-JF-R-011 and 16-JF-R-020 v. 3 and 4) and were in compliance with the Public Health Service Policy on Humane Care and Use of Laboratory Animals and the NIH Guide for the Care and Use of Laboratory Animals. Male Sprague-Dawley rats ([H1a: (SD) CVF, approximate body weight of 200–275 g at arrival, were obtained from Hilltop Lab Animals, Inc. (Scottdale, PA). All animals were free of viral pathogens, parasites, mycoplasm, *Heliobacter* and cilia-associated respiratory bacillus. Animals were acclimated for one week and housed in ventilated micro-isolator units supplied with HEPA-filtered laminar flow air (Lab Products OneCage; Seaford, DE), with Teklad Sanichip and Teklad Diamond Dry cellulose bedding or Shepherd Specialty Paper's Alpha-Dri cellulose (Shepherd Specialty Papers; Watertown, TN) bedding instead of Diamond Dry. They were provided tap water and autoclaved HaCXan Teklad Global 18% protein rodent diet (Harlan Teklad; Madison, WI) *ad libitum*. Rats were housed in pairs under controlled light cycle (12 h light/12 h dark) and temperature (22–25 °C) conditions.

2.2. Crude oil vapor

The crude oil used in this investigation to generate vapor was provided by BP Exploration and Production, Inc. and was characterized in Walter et al., 2022. The oil is reference material associated with the 2010 Deepwater Horizon spill from the Macondo Well in Mississippi Canyon Block 252, *i.e.*, "surrogate oil," that is similar to the Macondo Well crude oil (details in Walter et al., 2022).

2.3. Crude oil vapor inhalation exposures

The crude oil vapor inhalation exposure system and conditions devised for these experiments were described in Walter et al., 2022. Male Sprague-Dawley rats were placed in a custom, whole-body exposure chamber and exposed either to a single 6-h inhalation exposure to 300 ppm total volatile organic compounds (VOC; acute exposure) or to a sub-chronic exposure to 300 ppm total VOC 6 h/d × 4 d/wk × 4 wk. Control animals were exposed to filtered air. End points were measured at 1 d, 28 d, and 90 d post-exposure. Total VOC concentration was measured in real time during the exposures, and adjustments were automatically made to maintain a constant total VOC level. Benzene, toluene, ethylbenzene and xylene concentrations were also monitored during inhalation exposures.

2.4. In vivo pulmonary mechanics

The purpose of these experiments was to determine the effects of COV inhalation on pulmonary mechanics. Pulmonary input impedance was assessed using a flexiVent (SciReq; Montreal, Canada) small animal ventilator system permitting forced oscillation. Rats were anesthetized with i.p. injection of ketamine HCl (100 mg/kg; Hospira, Inc.; Lake Forest, IL) and xylazine (10 mg/kg; AnaSed; AKORN Animal Health; Lake Forest, IL). After the trachea was exposed through a mid-line incision, a cannula was inserted into the trachea a distance of ~5 cartilage rings and tied in place. Animals were then ventilated (90 breaths/min; tidal volume, 8 ml/kg; positive end expiratory pressure, 3 cm H_2O). This system interrupts normal ventilation to apply a short, small-amplitude, broad-band volume perturbation at the airway opening. Using the flow and pressure measured at the airway opening, a measurement of pulmonary input impedance was calculated. This measurement was then fit to a model consisting of a Newtonian resistance connected to a constant-phase tissue compartment. Parameters from this model embody energy dissipation in the airways and tissue, and energy storage within the tissue, and can be interpreted in terms of ventilation heterogeneity *vs.* de-recruitment and inflammation in the conducting airways *vs.* changes in the lung periphery. The ECG was monitored for changes in heart rate and depth of anesthesia during the period of measurement of respiratory system resistance (Rrs), elastance (Ers), tissue damping (G), tissue elastance (H), Newtonian resistance (Rn) and hysteresivity (η). The rats were euthanized by exsanguination while anesthetized upon completion of the experiment.

2.5. In vivo airway reactivity to MCh

The purpose of these experiments was to determine whether COV inhalation affects airway reactivity to inhaled methacholine (MCh; Spectrum Chemical MFG Corp.; New Brunswick, NJ). Rats were anesthetized with ketamine HCl (100 mg/kg; Hospira, Inc.; Lake Forest, IL) and xylazine (10 mg/kg; AnaSed; AKORN Animal Health; Lake Forest, IL) given *via* i.p injection. A mid-line incision was made in the neck, the trachea was exposed, and a cannula was advanced into the lumen. Animals received supplemental ketamine HCl (50 mg/kg) by administering the drug topically to the exposed muscle in the neck just before placing the animal into the plethysmograph. Animals were placed on a warming bed in a plethysmograph for the assessment of lung resistance (R_L) and dynamic compliance (C_{dyn})[FinePointe RC; Data Sciences International (DSI); St. Paul, MN] and were ventilated using a digital rodent ventilator (Élan Series RC; DSI). Ventilation settings were: maximum mouth pressure, 40 cm H_2O; maximum tidal volume, 3 ml; and respiratory rate, 90 bpm. After recording baseline values of R_L and C_{dyn} and delivery of saline vehicle to obtain baseline values, MCh aerosols were delivered from 20 μl of solutions of the following concentrations: 0.1, 0.1725, 0.3, 1.0, 1.73, 3.0, 5.75, 10.0 and 17.25 mg/ml. Three, 5-ml (45 cm H_2O mouth pressure) deep inspirations were applied just before each MCh dose was delivered. Maximum R_L (R_{Lmax}) values and minimum C_{dyn} values (C_{dynmin}) were logged at 5-s intervals to quantify responses to MCh. Following completion of the experiment, the rats were sacrificed by exsanguination while under anesthesia.

2.6. In vitro reactivity to MCh: isolated, perfused trachea

The purpose of these experiments was to determine whether airway smooth muscle reactivity to MCh and the modulatory effect of the airway epithelium on reactivity were altered by COV inhalation. The isolated, perfused trachea preparation has been described in detail (Fedan and Frazer, 1992; Fedan et al., 2001). Rats were given an overdose of sodium pentobarbital (100–300 mg/kg, i.p.; Fatal Plus; Vortec Pharmaceuticals LTD; Dearborn, MI) and euthanized by exsanguination. A 25-mm segment of trachea was removed, cleaned and mounted on a perfusion holder at its *in situ* length. The holder contained indwelling, side-hole catheters in the lumen that were connected to the positive (inlet) and negative (outlet) sides of a differential pressure transducer. The holder, with mounted trachea, was placed into an extraluminal (EL) bath containing modified Krebs-Henseleit solution (MKHS). MKHS (pH 7.4, 37 °C) contained 113 mM NaCl, 4.8 mM KCl, 2.5 mM $CaCl_2$, 1.2 mM KH_2PO_4, 1.2 mM $MgSO_4$, 25 mM $NaHCO_3$, and 5.7 mM glucose, and was saturated with 95% O_2/5% CO_2. The trachea was perfused at a constant rate (25 ml/min) with MKHS from a separate bath, the intraluminal (IL) bath, while measuring inlet minus outlet pressure difference (△P, cm H_2O) as an index of tracheal diameter. Transmural pressure was set to zero. The MHKS in the IL and EL baths was replaced at 15-min intervals with fresh solution, followed by a 30-min equilibration period in which the MHKS was not changed and the baseline was allowed to become stable. After the equilibration period, MCh (Sigma-Aldrich; St. Louis, MO) was added in stepwise-increasing, cumulative concentrations to the

EL bath to induce contractile responses for the generation of concentration-response curves. At the conclusion of the EL concentration-response determination, the EL and IL MKHS was changed at 15-min intervals. Ninety min after the conclusion of the EL concentration-response determination, stepwise-increasing, cumulative concentrations of MCh were added to the IL bath. Thus, a paired design was employed for each trachea.

The results of the isolated, perfused trachea experiments are presented in several ways: 1) the -log[EC50 (M)] values for MCh applied to the EL and IL baths are given along with the maximum contractile responses in terms of △P (cm H_2O), 2) the EL and IL concentration-response curves are shown with responses normalized in terms of the maximum responses obtained after EL and IL MCh additions (% maximum response), and 3) IL concentration-response curves are presented in a normalized fashion, in which the individual responses evoked in response to the IL additions of MCh are normalized with respect to the maximum response obtained after MCh was added extraluminally (% EL maximum response). The basis for the latter method of data expression is the fact that the normal relationship between the EL and IL curves is such that the IL curve is normally located to the right of the EL curve over the MCh concentration range, and the IL maximum reponse is smaller than the EL maximum response (Fedan and Frazer, 1992). Treatments that affect epithelial integrity or epithelium-derived relaxing factor (EpDRF) release alter the relationship between the two curves (Fedan et al., 2000), *i.e.*, damage to the epithelium is manifested as a leftward shift of the IL concentration-response curve and upward shift of the maximum response, whereas a change in smooth muscle reactivity is manifested as a change in the EC50 and maximum response to EL-applied MCh.

2.7. Electric field stimulation (EFS) of effector nerves

In the rat, airway diameter is under the regulation of cholinergic motor nerves. The purpose of these experiments was to ascertain whether COV exposure affected effector nerve function by eliciting excitatory neurotransmitter release with EFS (Fedan et al., 2001). Rats were given an overdose of sodium pentobarbital (100–300 mg/kg, i.p.; Fatal Plus) and euthanized by exsanguination. A segment of trachea was removed, cleaned, and segments, two-cartilage-rings wide, were prepared. Every effort was made to avoid damage to the epithelium. The rings were opened by cutting through the cartilage rings opposite the smooth muscle layer to prepare "strips," and suture was attached to each cut end of the cartilage segments. One end of the strip was attached to the electrode holder, the other end was attached to a force-displacement transducer for the measurement of isometric force. The holder containing the strip was placed in an organ chamber containing MKHS. When attached to the holder, the strip had been situated between two platinum ring electrodes, at either end of the strip, for the delivery of electric field stimulation. The strips were placed under 0.6 g basal tension. After a 1.5-h equilibration period, the preparations were stimulated with 10-s trains of square-wave pulses of 120 V and 0.5 msec duration and increasing frequency to develop frequency-response curves for the development of contractile responses. There were 5 min between stimulation periods. At the conclusion of the frequency-response determination, the preparations were contracted with 120 mM KCl, and the individual contractions of each tracheal strip were normalized as percentage of the response to KCl (% KCl). In preliminary experiments, preparations were pre-contracted with 3×10^{-6} M MCh (Sigma-Aldrich) to determine whether relaxation responses could be evoked by stimulation of inhibitory nerves (Fedan et al., 2001); in those experiments relaxation responses were not observed. Thus, in rat trachea only cholinergically-mediated contractile responses were elicited by EFS.

2.8. Epithelial ion transport in isolated tracheal segments

In order to ascertain whether exposure to COV interfered with airway epithelial ion transport, after giving an overdose of sodium pentobarbital (100–300 mg/kg, i.p.; Fatal Plus) and euthanasia by exsanguination, tracheal segments were removed from animals, cleaned, and mounted in Ussing chambers in order to measure transepithelial potential difference (V_t; mV), transepithelial resistance (R_t), and short-circuit current (I_{sc}). The apical and basolateral chambers of the apparatus contained MKHS solution. The epithelium was allowed to reach a stable V_t under open-circuit conditions before applying a 0-mV voltage-clamp across Ag/AgCl electrodes (4% agar in MKHS) in order to record I_{sc} (μA/cm^2), an index of active ion transport, using an EVC 4000 automatic voltage/current amplifier (World Precision Instruments; Sarasota, FL). Square-wave voltage pulses (1 mV, 5 s duration) were delivered every 55 s to yield a voltage response for calculation of R_t, an index of paracellular permeability, from Ohm's law.

To investigate the possible involvement of COV-induced changes in epithelial Na^+ and Cl^- channels and the Na^+,K^+-pump, the effects of the following inhibitors were evaluated: apical amiloride (3×10^{-5} M, apical chamber) to block apical membrane Na^+ channels, apical 5-nitro-2-(3-phenylpropylamino) benzoic acid (NPPB; 10^{-4} M, apical chamber) to block apical membrane Cl^- channels, and ouabain (10^{-4} M; basolateral chamber) to block the basolateral membrane Na^+,K^+-pump. The responses to these agents were quantified with regard to their effects on I_{sc} and R_t. Amiloride was dissolved in saline; NPPB and ouabain were dissolved in dimethyl sulfoxide (DMSO). All inhibitors were from Sigma-Aldrich (St. Louis, MO).

2.9. Measurement of vascular permeability using Evans blue dye

The purpose of these experiments was to investigate the effects of COV exposure on vascular permeability of airway blood vessels using capsaicin-induced Evans blue dye extravasation. Evans blue dye binds tightly to albumin after i.v. injection and appears in extravascular tissues if vascular permeability is increased; Evans blue normally remains in the vascular compartment after it is injected intravenously.

Following an i.p. injection of ketamine HCl (100 mg/kg) plus xylazine (50 mg/kg), a ventral, left of midline neck incision was used to isolate and cannulate the jugular vein. Stock capsaicin (USP; Sigma-Aldrich) was prepared by dissolving 7.5 mg capsaicin in 0.75 ml of ethanol and 0.25 ml Tween 80 and then diluting with 99 ml of normal saline. Evans blue dye (30 mg/kg) was infused i.v. (external jugular vein) followed 5 min later by an i.v. injection of capsaicin (75 μg/kg). Five min after capsaicin, the rat was perfused with normal saline for 2 min at 0.25 ml/g. An identical protocol was used for non-capsaicin controls using normal saline in place of capsaicin. Two experimental approaches were used: In the acute COV study, control animals did not receive capsaicin; in the sub-chronic COV study, control animals received capsaicin to determine if basal permeability was affected by COV. Five min after capsaicin was given, the abdomen was opened, the rat was exsanguinated, and the thoracic aorta was catheterized retrogradely. The inferior vena cava was tied off to limit perfusion to the upper body and a small hole was cut in the left atrium. The animal was perfused with 0.25 ml/g saline over 2 min to flush excess dye from the bronchial and pulmonary vasculature. The trachea, intrapulmonary airways and lung were removed, and Evans blue was extracted in formamide. Evans blue level was measured in a photometer at 620 nm, calibrated to a standard curve, and recorded as mg Evans blue/mg wet tissue.

2.10. Statistical analysis

The results are expressed as means±SEM. For airway reactivity to MCh *in vivo* experiments, and isolated, perfused trachea and Ussing chamber experiments performed using excised tracheas, the results were analyzed for differences using analysis of variance (ANOVA). Effective MCh concentrations (M) giving 50% of the maximum response (EC50) in isolated, perfused trachea experiments were calculated for each

concentration-response using a 4-parameter logit curve fit and transformed to give logarithmically-transformed values, which are normally distributed; these results are expressed as logEC50 (M). Area under the curve (AUC) analysis was conducted for the % EL maximum parameter. The remaining results were analyzed using JMP version 13.2 for Windows. Dependent variables were analyzed using two-way analyses of variance (treatment by day). Post-hoc pairwise comparisons between treatments on the same day were evaluated from the full model using Students *t*-tests. For all analyses $P < 0.05$ was regarded as significant.

3. Results

3.1. In vivo pulmonary mechanics

To evaluate the effects of acute and sub-chronic COV inhalation, respiratory system resistance (Rrs), elastance (Ers), tissue damping (G), tissue elastance (H), Newtonian resistance (Rn) and hysteresivity (η) were measured. Following acute inhalation, no effects of COV on any of these six parameters were observed 1 or 28 d post-exposure (Supplementary Fig. 1). To determine if sub-chronic inhalation of COV and more extended post-exposure periods might reveal changes in lung mechanics, the animals were examined 1, 28 and 90 d post-exposure. Again, no significant effects of COV exposure were observed (Supplementary Fig. 2). COV, therefore, had no effects on pulmonary mechanics after acute or sub-chronic inhalation exposures.

3.2. In vivo airway reactivity to MCh

The effects of COV inhalation on *in vivo* reactivity to inhaled MCh aerosol following acute and sub-chronic exposures were investigated. Neither basal R_L nor basal C_{dyn} were affected 1 d and 28 d following acute exposure to COV (Supplementary Fig. 3). The subsequent inhalation delivery of MCh to induce bronchoconstriction did not reveal an effect of COV treatment on reactivity to this bronchoconstrictor, either in terms of R_L or C_{dyn} responses (Supplementary Fig. 4). While not at 1 or 28 d post-exposure, basal R_L was elevated significantly 90 d after the end of sub-chronic inhalation; basal C_{dyn} was not changed (Fig. 1). Reactivity to MCh was not affected at any post-exposure end point, in terms of R_L or C_{dyn} responses (Supplementary Fig. 5).

3.3. In vitro airway reactivity to MCh

The isolated, perfused trachea preparation was employed in this series of experiments to evaluate whether inhaled COV affects airway smooth muscle reactivity to MCh and/or the diffusion barrier/modulatory effect of the airway epithelium on reactivity. The effects of both acute and sub-chronic exposures were examined.

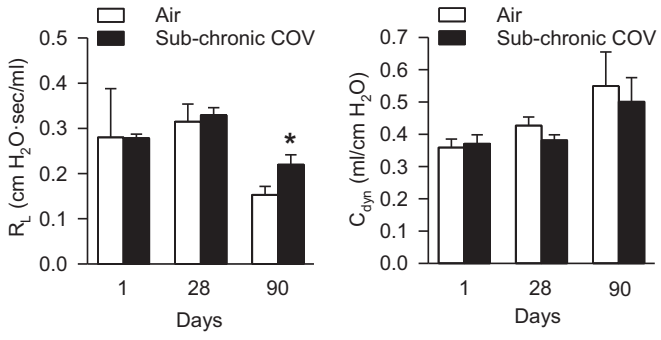

Fig. 1. Effect of sub-chronic inhalation of 300 ppm COV for 28 d on basal R_L and C_{dyn} 1, 28 and 90 d post-exposure. *n* values were as follows: for 1 d post-exposure, air control, $n = 8$, and COV, $n = 6$; for 28 d post-exposure, air control, $n = 7$, and COV, $n = 5$; for 90 d post-exposure, air control, $n = 6$, and COV, $n = 8$. COV increased basal R_L at 90 d post-exposure.

EL and IL concentration-response curves for MCh-induced contraction of the preparations, both obtained in each trachea from four groups of rats 1 or 28 d following acute exposure to air or COV, and 1, 28 and 90 after sub-chronic exposure, are depicted in Figs. 2 and 3, respectively. The figures depict the rightward and downward location of the IL curves in comparison with the EL curves. The -logEC50 values for the EL and IL curves from air- and COV-exposed tracheas are presented in Table 1 and the associated concentration-response curves are depicted in Supplementary Figs. 6 and 7. Neither acute nor sub-chronic COV affected reactivity to EL- or IL-applied MCh, *i.e.*, -logEC50 values for MCh.

In the isolated, perfused trachea preparation, △P (cm H_2O) varies with the 5th power of the radius. The initial diameter of the trachea while in the apparatus, under a standard, fixed rate of perfusion with MKHS through the lumen, sets the basal value of △P, which is then beyond the control of the investigator. Responses to a given contractile agonist are enlarged in preparations with a high basal △*P* value compared to those with low △*P* values. To evaluate further whether exposure to COV altered the relationship between EL and IL MCh concentration-response curves [see Fedan and Frazer (1992)], the results were expressed in terms of the IL responses to MCh normalized in terms of the respective EL maximum responses obtained from the same preparation, *i.e.*, % EL maximum response. In Figs. 2 and 3, the response values in the IL curve labelled "a" were divided by the maximum EL response, labelled "b," and multiplied by 100. The results of this analysis are given in Figs. 4 and 5. Acute exposure to COV had no effect on the % EL maximum response concentration-response relationships obtained at 1 d post-exposure, but reduced the magnitude of responses 28 d post-exposure at two MCh concentrations: 3.48×10^{-5} and 10^{-4} M MCh (Fig. 4). After sub-chronic treatment a significant reduction in the % EL maximum response occurred at 90 d post-exposure (Fig. 5). Both changes are indicative of an increased inhibitory effect of the epithelium on IL reactivity to MCh.

3.4. EFS of effector nerves

Following acute or sub-chronic inhalation of COV no effects on EFS-induced contractile responses of tracheal strips were detected at any post-exposure end point (Supplementary Fig. 9), suggesting that cholinergic regulation of the airways was not affected by COV exposure.

3.5. Epithelial ion transport in isolated tracheal segments

The effects of acute and sub-chronic COV inhalation on basal tracheal epithelial ion transport and the effects of ion transport inhibitors was investigated *in vitro*. Acute COV inhalation (Fig. 6) had no effect on baseline I_{sc} and R_t 1 d post-exposure nor on responses to amiloride, NPPB and ouabain. Twenty-eight d following acute COV inhalation no effects on the responses to amiloride, NPPB and ouabain were observed, with the exception of a significant decrease in the % decrease in R_t following administration of NPPB; this change is not regarded as being meaningful biologically.

One d following sub-chronic exposure to COV R_t was significantly elevated, indicative of a decline in paracellular ion permeability (Fig. 7). Two modest but significant changes were noted at 28 d post-exposure, *i.e.*, an increase in the response to NPPB (that is, a greater decrease in I_{sc}), which could signify an up-regulation of active Cl^- transport, and an increase in the response to amiloride, which could signify an increase in active Na^+ transport. No changes in ion transport characteristics were observed 90 d post-exposure.

3.6. Vascular permeability

Supplementary Fig. 10 describes the effect of acute COV exposure on capsaicin-induced Evans blue extravasation responses in trachea, bronchus and lung tissue 1 and 28 d post-exposure. In this series of experiments control animals were not administered capsaicin. Generally, COV

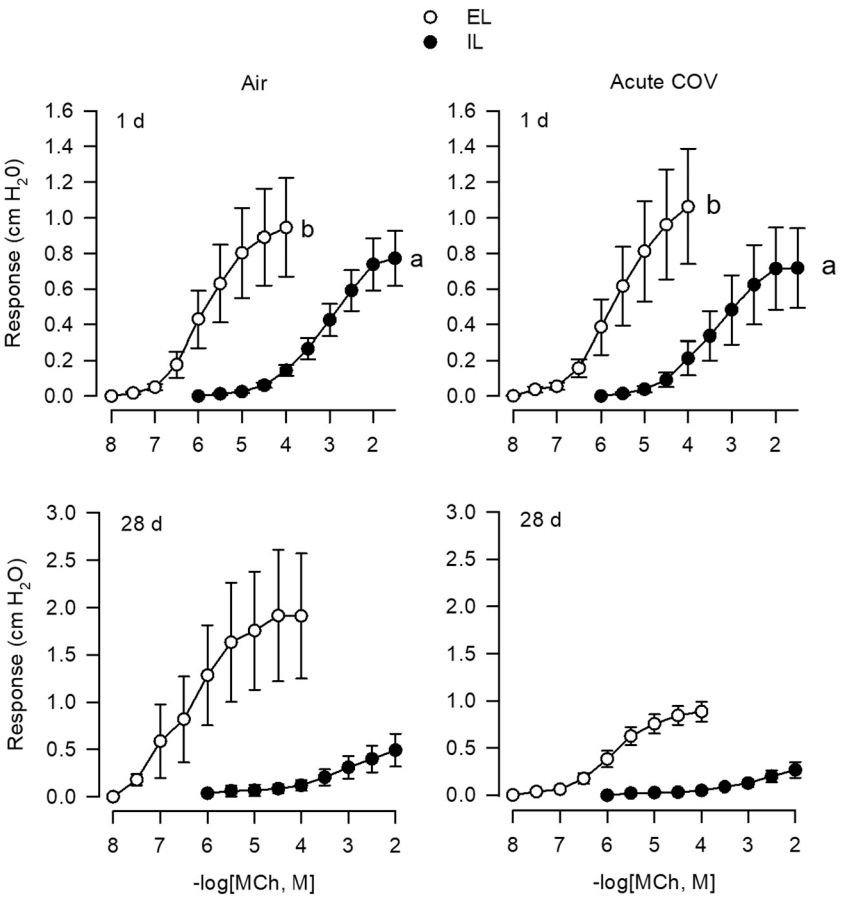

Fig. 2. Effect of acute inhalation of 300 ppm COV on *in vitro* reactivity to MCh in the isolated, perfused trachea preparation 1 and 28 d post-exposure, showing cumulative concentration-response curves for MCh applied to the EL bath and IL bath. The IL concentration-response curves were displaced to the right of the EL curves, and the maximum responses to IL-administered MCh were reduced in size compared to those generated after EL MCh application 28 d post-exposure. *n* values were as follows: for 1 d post-exposure, air control EL, $n = 6$, and COV, $n = 7$; air control IL, $n = 6$, and COV, $n = 6$; for 28 d post-exposure, air control EL, $n = 9$, and COV, $n = 8$; 28 d post-exposure IL, air control, $n = 6$, and COV, $n = 6$. "b" and "a" refer to the maximum responses to extraluminally-applied and intraluminally-applied MCh, from which the parameter, % EL maximum response, was calculated (also see Fig. 3).

appeared to decrease extravasation in all three regions and at all post-exposure end points. However, these effects were not significant. Likewise, there were no differences in the responses to capsaicin at 1 and 28 d in the air-exposed groups and in the COV-exposed groups.

In the experiments involving sub-chronic exposure to COV, it was decided to expand the experimental matrix to ascertain whether COV treatment alone had an effect on extravasation. The results are shown in Supplementary Fig. 11, wherein it can be seen that COV exposure had no effect on basal vascular permeability at any time point in any region of the lung. The stimulatory effect of capsaicin is also shown in the figure, and this effect occurred to varying degrees in all the lung regions at the three end point times. However, there were no significant differences in the effects of capsaicin that could be attributed to treatment with COV in any lung region or end point time.

4. Discussion

In this study several methods were utilized to evaluate the ventilatory and non-ventilatory effects of inhalation of COV in the lungs of rats. Both acute and sub-chronic exposures to COV were employed to model different exposure scenarios in the workplace: the acute exposure to mimic a one-time exposure of a worker, and the sub-chronic exposure to mimic a more protracted exposure. The end point times were chosen to detect a possible recovery (1 and 28 d post-exposure) from effects after a single exposure, whereas it was reasoned that sub-chronic exposure effects would require longer periods of time (1, 28 and 90 d) for pulmonary effects to become reversed. The results of this study in aggregate indicate that neither acute nor sub-chronic inhalation exposures to COV elicited substantive toxicity in the rat lung at any post-exposure time point. In addition, changes when observed appear to be reversible in time, with the exception of those related to R_L and epithelial modulation of airway reactivity to MCh *in vitro*.

Among the analyses undertaken, pulmonary mechanics measurements (forced oscillation technique) revealed no changes in respiratory system resistance, elastance, tissue damping, tissue elastance, Newtonian resistance and hysteresivity. Curiously, even though respiratory resistance and elastance did not change, a significant increase occurred 90 d after the sub-chronic exposure as assessed using an analogous parameter, R_L (plethysmography technique). An explanation for this difference is not readily apparent. Nor is it clear why no changes in R_L occurred at earlier end points when taking plethysmographic measurements over a 90-d period. However, it does suggest the possibility that a degree of breathing difficulty could accompany extended exposure of workers to COV. Nevertheless, reactivity of the airways to inhaled MCh aerosol, measured either in terms of R_L or C_{dyn}, was not affected. Together, these findings indicate that inhalation of 300 ppm COV acutely or sub-chronically for 28 d or less is without severe impact on pulmonary function or airways reactivity to MCh in the rat. They also suggest that pathophysiological alterations may be triggered that become manifested at later times as an increase in airway resistance. Additional studies will be needed to investigate whether airway resistance becomes heightened further beyond 90 d *in vivo*.

Recently, Amor-Carro et al. (2020) investigated the effects of inhalation of vapor from a synthetic analogue of class 2B fuel oil released from the oil tanker MV *Prestige* in three animal models, two in rat and one in mouse. Following inhalation exposure to vapor 2 h/d × 5 d/wk× 3 wk. and measurement of airway resistance changes in response to inhaled MCh using a flexiVent system, the authors observed that the Wistar and Brown-Norway strains of rats developed airway hyperreactivity to MCh immediately after and 2 wk. after the end of the exposure. Airway hyperreactivity did not develop in the mice, however. The vapor was delivered from a 60 °C source and the level delivered to the animals

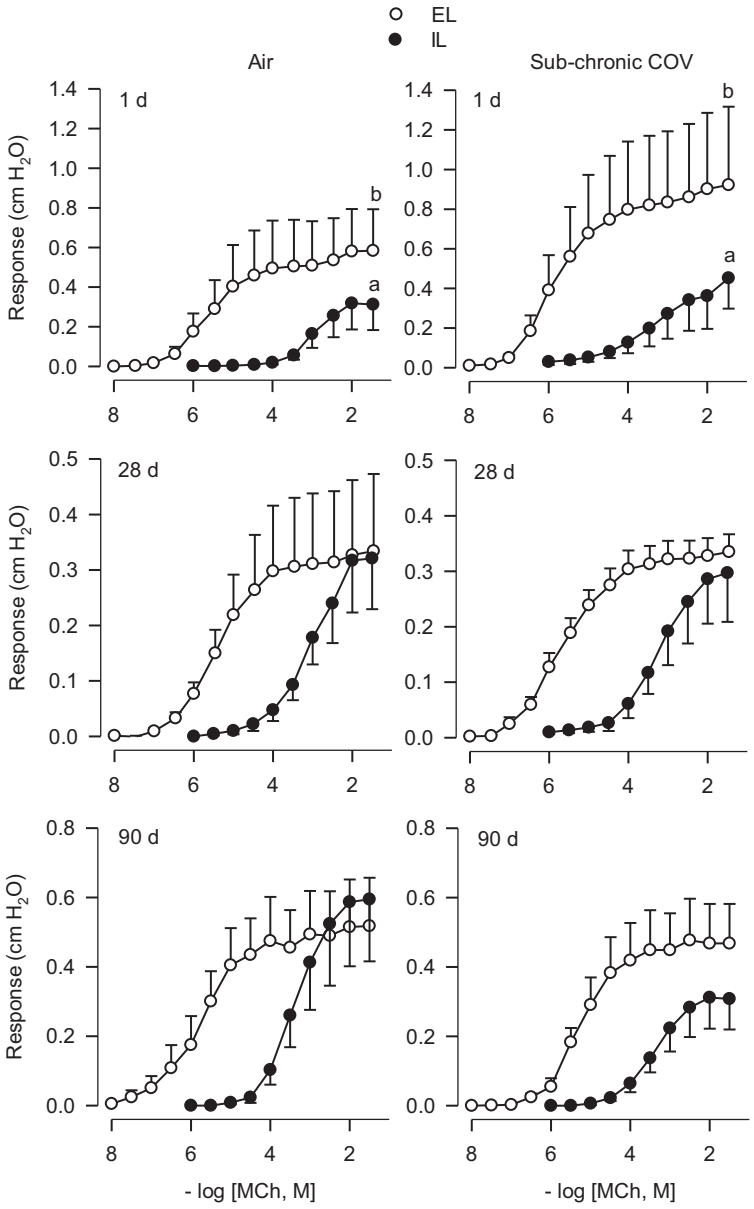

Fig. 3. Effect of sub-chronic inhalation of 300 ppm COV on *in vitro* reactivity to MCh in the isolated, perfused trachea preparation 1, 28 and 90 d post-exposure, showing cumulative concentration-response curves for MCh applied to the EL bath and IL bath. The IL concentration-response curves were displaced to the right of the EL curves, and the maximum responses to IL-administered MCh were reduced in size compared to those generated after EL MCh application 28 d post-exposure. *n* values were as follows: for 1 d post-exposure, air control EL and IL, $n = 6$, and COV, $n = 6$; for 28 d post-exposure, air control EL, $n = 6$, and COV, $n = 6$; air control IL, $n = 5$, and COV, $n = 5$; for 90 d post-exposure, air control EL and IL, $n = 3$, and COV, $n = 5$. "b" and "a" refer to the maximum responses to extraluminally-applied and intraluminally-applied MCh, from which the parameter, % EL maximum response, was calculated; also see Fig. 2.

Table 1
Reactivity of isolated, perfused trachea to MCh added to the extraluminal or intraluminal bath following inhalation of filtered air or 300 ppm COV.

Treatment	Days Post-exposure	-log[EC50 (M)]	
		Extraluminal	Intraluminal
Acute COV			
Filtered air	1	5.25 ± 0.08 (6)	3.14 ± 0.15 (6)
COV-exposed	1	5.76 ± 0.19 (6)	3.11 ± 0.24 (5)
Filtered air	28	6.27 ± 0.20 (9)	2.98 ± 0.23 (6)
COV-exposed	28	6.09 ± 0.13 (8)	2.94 ± 0.10 (5)
Sub-chronic COV			
Filtered air	1	4.93 ± 0.39 (6)	2.84 ± 0.18 (6)
COV-exposed	1	5.48 ± 0.16 (6)	2.87 ± 0.20 (7)
Filtered air	28	6.54 ± 0.57 (6)	3.40 ± 0.26 (5)
COV-exposed	28	5.68 ± 0.13 (6)	3.18 ± 0.12 (5)
Filtered air	90	5.85 ± 0.28 (5)	3.45 ± 0.20 (3)
COV-exposed	90	5.85 ± 0.07 (4)	3.24 ± 0.12 (5)

n in parentheses.

was not specified. In the present investigation, which utilized using Sprague-Dawley rats (see Sager et al., 2022) and inhalation of Deepwater Horizon surrogate oil, inflammation in the lung was not observed, a finding also reported by Amor-Carro et al. (2020).

The effects of fog (0.5 and 1.5 mg/l) generated from light weight lubricating oil on the lung following inhalation by rats for 4 or 13 wk were examined by Selgrade et al. (1987, 1990). Alveolar macrophage accumulation and elevation of polymorphonuclear leukocytes occurred following treatment. Several parameters related to pulmonary function were not, however, affected. These responses waned over a 4-wk post-exposure period and were considered mild.

Possible changes in reactivity in response to COV inhalation were also investigated in the present study under more controlled *in vitro* conditions using the isolated, perfused trachea. After application of MCh to the EL or IL baths to elicit contraction of the airway smooth muscle, the EC50 values for the bronchoconstrictor were not affected, which indicates that the sensitivity of the preparations to the agonist was not changed. This finding is in agreement with the lack of changes in airway reactivity to inhaled MCh. An interesting change in responsiveness to

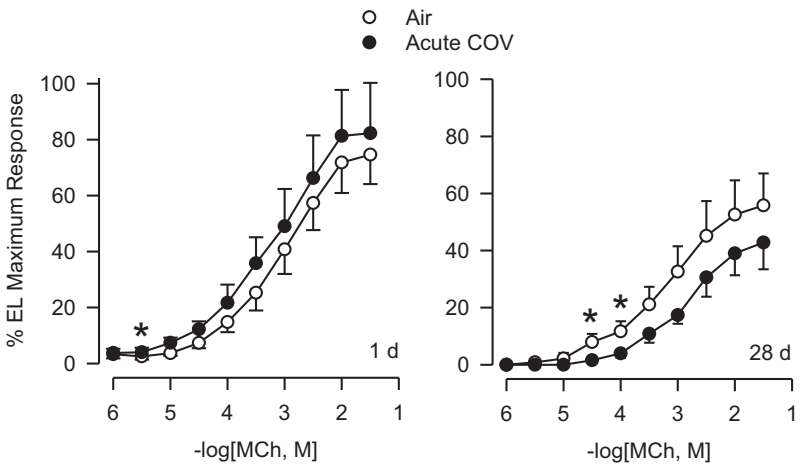

Fig. 4. Effect of acute inhalation of 300 ppm COV on *in vitro* reactivity to MCh in the isolated, perfused trachea preparation 1 and 28 d post-exposure showing cumulative concentration-response curves for MCh applied to the IL bath. The results shown here were calculated from those shown in Fig. 2 and indicate the magnitude of the responses to intraluminally-applied MCh expressed as a percentage of the maximum response to extraluminally-applied MCh in the same trachea; both curves were obtained from each trachea. *n* values were as follows: for 1 d post-exposure, air control, $n = 6$, and COV, $n = 6$; for 28 d post-exposure, air control, $n = 5$, and COV, $n = 4$. *Air *vs.* acute COV, $P < 0.05$.

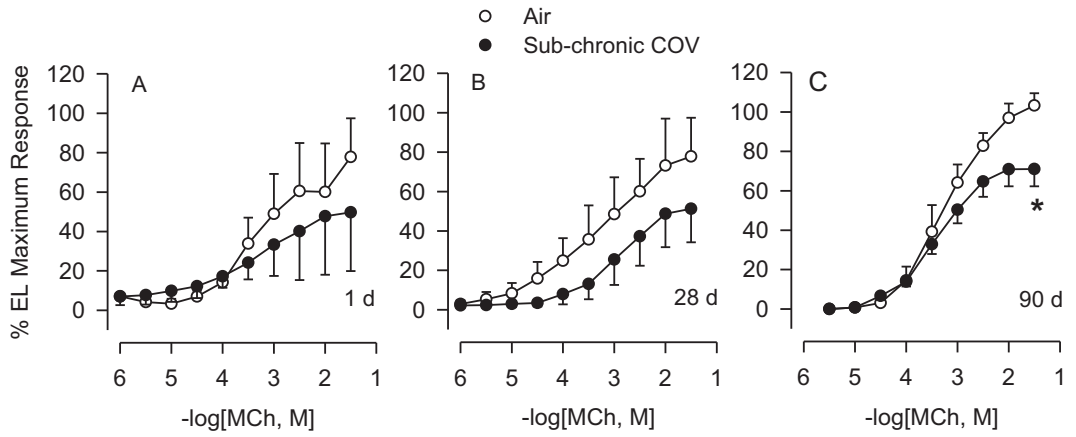

Fig. 5. Effect of acute inhalation of 300 ppm COV on *in vitro* reactivity to MCh in the isolated, perfused trachea preparation 1, 28 and 90 d post-exposure showing cumulative concentration-response curves for MCh applied to the IL bath. The results shown here were calculated from those shown in Fig. 7 and indicate the magnitude of the responses to intraluminally-applied MCh expressed as a percentage of the maximum response to extraluminally-applied MCh in the same trachea; both curves were obtained from each trachea. *n* values were as follows: for 1 d post-exposure, air control, $n = 6$, and COV, $n = 5$; for 28 d post-exposure, air control, $n = 4$, and COV, $n = 4$; 90 d post-exposure, air control, $n = 3$, and COV, $n = 5$. No differences in the magnitude of the responses were detected at 1 and 28 d post-exposure. *The maximum response of tracheas from COV-exposed animals was reduced significantly 90 d post-exposure compared to the air-breathing controls.

MCh was evident following its application to the IL bath, namely, responses to MCh (% EL maximum response) were decreased at 28 post-exposure to acute COV and 90 d post-exposure to sub-chronic COV treatments. This is a hallmark that airway epithelial function was altered. The change was not due to a generalized change in the epithelial permeability barrier, as the ED50s for MCh after intraluminal application was not affected by COV and R_t was increased at this end point rather than decreased. Rather, it is a reflection of a physiological antagonism attributable to an accentuated release of EpDRF (Fedan et al., 2001; Johnston et al., 2004). This finding contrasts with the absence of changes in reactivity to inhaled MCh. We speculate that in the absence of integrative reflexes engaged in the *in vivo* response to inhaled MCh, the greater inhibitory effect of the airway epithelium in the decentralized perfused trachea *in vitro* became detectable.

The cholinergic nerves in the airways of rats subserve bronchoconstriction. The results indicate that COV did not target their function *in vitro*, inasmuch as no effects on neurogenic contractile responses of tracheal strips were observed. The neuropeptidergic, substance P-containing sensory nerves in the airway also were unaffected by COV treatment. Capsaicin releases substance P from these nerves, which interacts with specific receptors and then elicits neurogenic inflammation that results in increased vascular permeability. The finding that no differences in capsaicin-induced Evans blue leakage occurred after COV exposure signifies that the release of substance P from sensory nerves or its agonist activity was not affected by COV. Thus, intramural motor and sensory nervous control of the airways was uncompromised by COV. In addition, in the absence of challenge with capsaicin the basal levels of Evans blue leakage from vessels were similar in air-exposed and COV-exposed rats, suggesting that COV treatment alone did not affect vascular permeability in the lungs.

Ion transport by airway epithelium is critical to the maintenance of the airway surface liquid in which cilia beat to clear substances from the lungs. Therefore, the effect of COV exposure on ion transport was investigated. After the acute exposure to COV there were no effects on basal levels of I_{sc} and R_t at the 1 and 28 d end points or on responses to amiloride, NPPB and ouabain, save a small change in R_t (% change in R_t) associated with the response to NPPB that is probably not biologically meaningful. A variety of changes followed sub-chronic COV exposure.

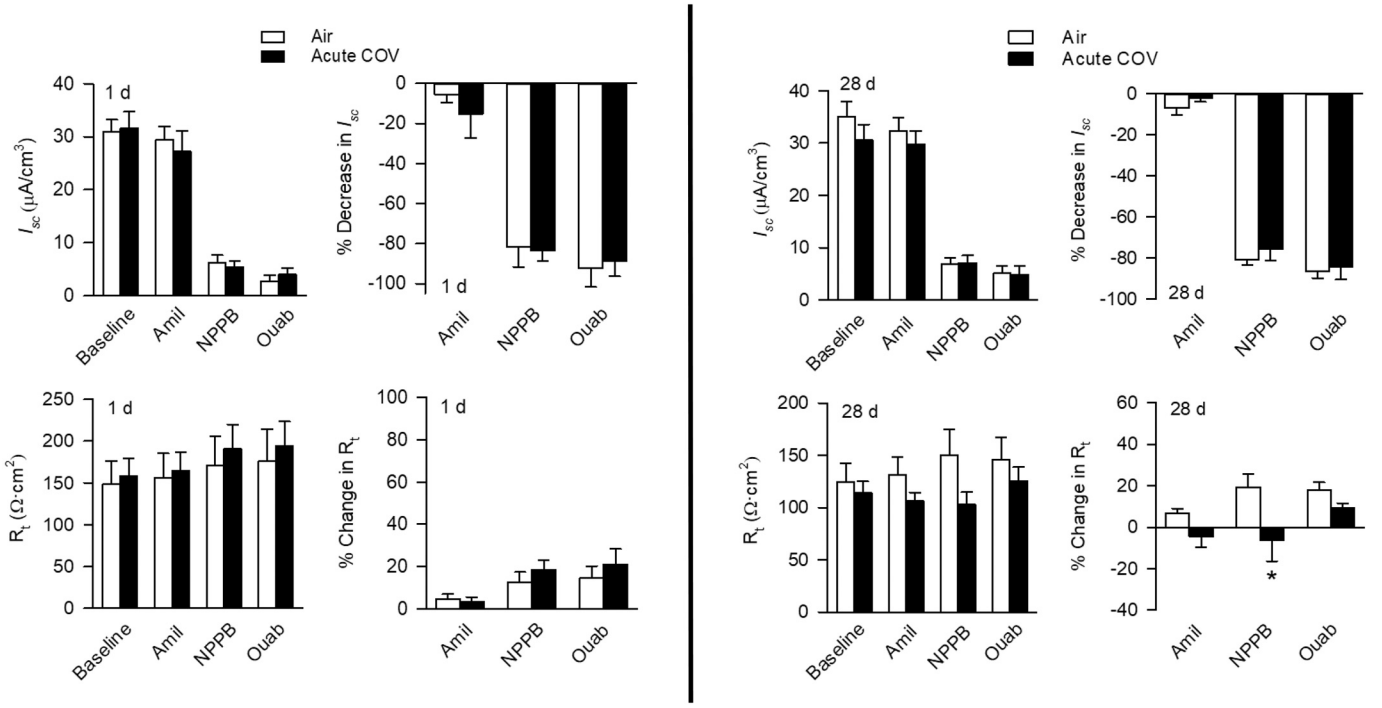

Fig. 6. Effect of acute 300 ppm COV inhalation exposure on basal parameters and bioelectric responses of tracheal epithelium to amiloride (3×10^{-5} M) and NPPB (10^{-4} M) in Ussing chambers *in vitro*. The results plotted to the left of the dark vertical line were obtained 1 d after acute COV exposure; the results to the right of the line are results obtained 28 d after acute exposure to COV. There were no effects of COV on I_{sc} or R_t at either time point, with the exception of a small but significant decrease in R_t during the response to NPPB at 28 d post-exposure to COV. *n* values were as follows: for 1 d post-exposure, air control, $n = 7$, and COV, $n = 6$; for 28 d post-exposure, air control, $n = 8$, and COV, $n = 7$. $^*P < 0.05$.

One d post-exposure basal R_t was increased, and the transport blockers did not affect R_t further. A likely explanation for this change is a decrease in the transepithelial, paracellular transport of Na^+ coupled to Cl^-, apical to basolateral, which would increase hydration of the airway surface liquid. These changes were not observed 28 and 90 d post-exposure. Instead, the results suggest that the electrogenic transport of Na^+ and Cl^- through their respective channels was increased modestly, as judged by the greater effects of NPPB and amiloride. If real, these changes are contradictory, because an increase in Cl^- transport would hydrate the airway surface liquid, whereas an increase in Na^+ transport would have the opposite effect. The results indicate that that normal electrogenic ion transport was restored by 90 d post-exposure.

Field studies by NIOSH investigators have included air monitoring measurements of VOC levels in a number of workplace scenarios. During transfer of petroleum condensate from a storage tank onto a truck, gases and vapors released into the air near the truck exceeded 348,000 ppm, and the concentrations of gas/vapors of methane, ethane, propane, and butanes exceeded levels that are immediately dangerous to life or health (IDLH; Retzer et al., 2018). During tank gauging tasks, peak short-term levels of VOC were above 2000 ppm and sustained levels as high as 500 ppm were observed. Gauging through thief hatches has led to several worker deaths resulting from inhalation of very high levels (> 100,000 ppm; National Institute for Occupational Safety and Health/Occupational Safety and Health Administration, 2015; Jordan, 2015) of VOC. The present study did not attempt to model these events. Instead, it attempted to understand the effects of VOC in other workplace scenarios that are more routine in upstream oil processing. For example, monitoring of tank gauging activities identified instances of peak concentrations of flammable gas and vapors as high as 40% of the lower explosive limit (LEL). Peak short-term levels of total VOCs were above 2000 ppm. and sustained levels as high as 500 ppm were measured. The COV level to which the animals were exposed by inhalation in this study was 300 ppm, which is in the range of many worker exposures and far below the extreme levels that have been reported and/or associated with deaths of workers. There is no "typical" level to which workers in all job categories are exposed, based on personal breathing zone measurements (Esswein et al., 2014a). Our study was designed to obtain insights into the effects of COV in the lungs of workers who are exposed on an acute and regular regular basis. A deficiency in the animal model used is its inability to capture all the workplace scenarios that occur on a daily basis, for example, the intermittency of the exposures, weather conditions, and other mitigating factors that are difficult to capture in the exposure design. Nevertheless, COV was observed to possess some bioactivity in ventilatory and non-ventilatory functions in the lung which, over the time spans studied, appear to be reasonably minor and reversible. As there is little or no clinical information about the effects of COV in workers, save its lethal effects, this study provides justification for worker surveillance in the upstream segment. Long-term respiratory ailments have been reported in Coast Guard responders to the Deepwater Horizon oil spill incident, but these individuals were exposed to oil that had been weathered by the sea and the environment (Rusiecki et al., 2018; Alexander et al., 2018).

Another limitation of the present study is attributable to the route of COV exposure, *i.e.*, whole body inhalation. The animals in the exposure chamber experienced dermal exposure as well as inhalation exposure. How dermal exposure might have contributed to the findings of this study cannot be determined at this level of investigation and will require future examination of the effects of COV inhalation administered using a nose-only inhalation system.

In conclusion, the findings indicate that acute and sub-chronic COV inhalation does not appreciably affect ventilatory properties of the rat, but transient changes in airway epithelium occur.

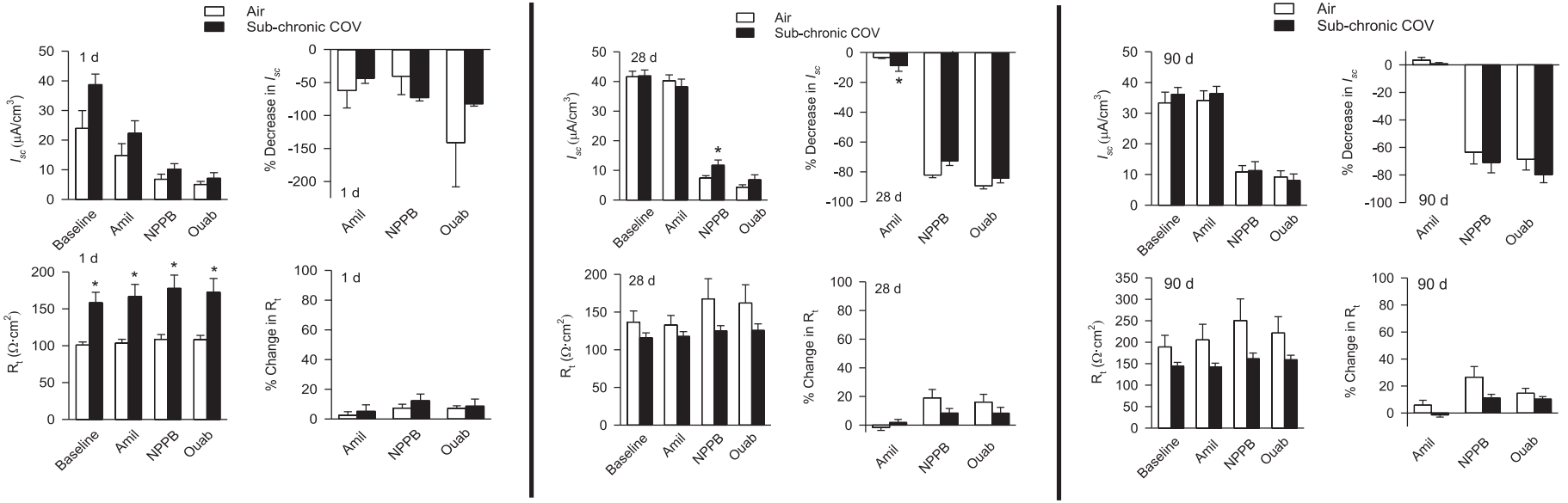

Fig. 7. Effect of sub-chronic 300 ppm COV inhalation exposure on basal parameters and bioelectric responses of tracheal tracheal epithelium to amiloride (3×10^{-5} M) and NPPB (10^{-4} M) in Ussing chambers *in vitro*. The group of graphs on the left hand side of the figure were obtained 1 d after sub-chronic COV exposure; the group of graphs in center of the figure were obtained 28 d after sub-chronic COV exposure; the group of graphs on the right hand side of the figure were obtained 90 d after sub-chronic COV exposure. At 1 d post-exposure basal R_t values were elevated both in the absence and presence of the transport inhibitors, indicative of an increase in paracellular resistance, whereas I_{sc} values were not affected. At 28 d post-exposure the decrease in I_{sc} induced by amiloride was significantly increased, and R_t values were unaffected. There were no effects of COV on I_{sc} or (R_t) 90 d post-exposure. *n* values were as follows: for 1 d post-exposure, air control, $n = 6$, and COV, $n = 6$; for 28 d post-exposure, air control, $n = 8$, and COV, $n = 8$; 90 d post-exposure, air control, $n = 7$, and COV, $n = 8$. No differences in the magnitude of the responses were detected at 1 and 28 d post-exposure. *$P < 0.05$.

5. Disclaimer

The findings and conclusions in this report are those of the authors and do not necessarily represent the official position of the National Institute for Occupational Safety and Health, Centers for Disease Control and Prevention. Mention of brand name does not constitute product endorsement.

Supplementary data to this article can be found online at https://doi.org/10.1016/j.taap.2022.116154.

Credit author statement

Jeffrey S. Fedan: Conceptualization, Data Curation, Visualization, Investigation, Supervision, Manuscript Writing, Reviewing and Editing; Janet A. Thompson: Methodology, Investigation, Data Curation, Editing; Kristen A. Russ, Methodology, Investigation; Richard D. Dey, Methodology, Investigation; Jeffrey S. Reynolds, Methodology, Investigation; Michael L. Kashon: Data Curation; Mark Jackson, Methodology; Walter McKinney: Conceptualization, Methodology, Investigation.

Declaration of Competing Interest

The authors declare that they have no known competing financial interests or personal relationships that could have appeared to influence the work reported in this paper.

Acknowledgements

Funding was provided by the National Institute for Occupational Safety and Health, Project Number 7927ZLDC.

References

Agency for Toxic Substances and Disease Registry, 1995. Toxicological Profile for Polyaromatic Hydrocarbons. www.atsdr.cdc.gov/toxprofiles/tp.asp?id=122&tid=25.

Agency for Toxic Substances and Disease Registry, 1999. Toxicological Profile for Total Petroleum Hydrocarbons (TPH). www.atsdr.cdc.gov/toxprofiles/tp.asp?id=424&tid=75.

Agency for Toxic Substances and Disease Registry, 2007. Toxicological Profile for Benzene. www.atsdr.cdc.gov/toxprofiles/tp.asp?id=40&tid=14.

Agency for Toxic Substances and Disease Registry, 2016. Toxicological Profile for Hydrogen Sulfide and Carbonyl Sulfide. www.atsdr.cdc.gov/toxprofiles/tp114.pdf.

Alexander, M., Engel, L.S., Olaiya, N., Wang, L., Barrett, J., Weems, L., 2018. The deepwater horizon oil spill coast guard cohort study: a cross-sectional study of acute respiratory health symptoms. Environ. Res. 162, 196–202.

Amor-Carro, Oscar, White, Kathryn M., Fraga-Iriso, Rebeca, Marinas-Pardo, Luis A., Nunez-Naveira, Laura, Lema-Costa, Beatriz, Villarnovo, Marta, Verea-Hernando, Hector, Ramos-Barbon, David, 2020. Airway hyperresponsiveness, inflammation, and pulmonary emphysema in rodent models designed to mimic exposure to fuel oil–derived volatile organic compounds encountered during an experimental oil spill. Environ. Health Perspect 128 (2), 027003-1–027003-14. https://doi.org/10.1289/EHP4178.

Centers for Disease Control and Prevention. National Institute for Occupational Safety and Health, 2020a. Fatalities in the Oil and Gas Extraction Industry (FOG). www.cdc.gov/niosh/topics/fog/default.html.

Centers for Disease Control and Prevention. National Institute for Occupational Safety and Health, 2020b. Fatalities in the Oil and Gas Extraction Industry (FOG). https://www.cdc.gov/niosh/topics/fog/publications.html.

Esswein, E.J., Snawder, J., King, B., Breitenstein, M., Alexander-Scott, M., Kiefer, M., 2014a. Evaluation of some potential chemical exposure risks during flowback operations in unconventional oil and gas extraction: preliminary results. J. Occup. Environ. Hyg. 11, D174–D184. https://doi.org/10.1080/15459624.2014.933960.

Esswein, E.J., Snawder, J., King, B., Breitenstein, M., Alexander-Scott, M., 2014b. Preliminary Field Studies on Worker Exposures to Volatile Chemicals during Oil and Gas Extraction Flowback and Production Testing Operations. https://blogs.cdc.gov/niosh-science-blog/2014/08/21/flowback-2/.

Fedan, J.S., 2022. Biological effects of inhaled crude oil vapor. I. Scope of the investigation. Toxicol. Appl. Pharmacol. (One of seven tandem papers submitted to TAAP).

Fedan, J.S., Frazer, D.G., 1992. Influence of epithelium on the reactivity of guinea-pig isolated, perfused trachea to bronchoactive drugs. J. Pharmacol. Exp. Ther. 262, 741–750.

Fedan, J.S., Millecchia, L.L., Johnston, R.A., Rengasamy, A., Hubbs, A., Dey, R.D., Yuan, L.X., Watson, D., Goldsmith, W.T., Reynolds, J.S., Orsini, L., Dortch-Carnes, J., Cutler, D., Frazer, D.G., 2000. Effect of ozone treatment on airway reactivity and epithelium-derived relaxing factor in guinea pigs. J. Pharmacol. Exp. Ther. 293, 724–734.

Fedan, J.S., Van Scott, M.R., Johnston, R.A., 2001. Pharmacological techniques for the in vitro study of airways. J. Pharmacol. Toxicol. Methods 45, 159–174.

Harrison, R.J., Retzer, K., Kosnett, M.J., Hodgson, M., Jordan, T., Kiefer, M., 2016. Sudden deaths among oil and gas extraction workers resulting from oxygen deficiency and inhalation of hydrocarbon gases and vapors - United States, January 2010 - March 2015. Morb. Mortal. Wkly Rep. 65, 6–9.

Investigative Team, 2022. Biological effects of inhaled crude oil vapor. VIII. Summary and conclusions. Toxicol. Appl. Pharmacol. (One of seven tandem papers submitted to TAAP).

Johnston, R.A., Van Scott, M.R., Kommineni, C., Millecchia, L.L., Dortch-Carnes, J., Fedan, J.S., 2004. Hyperosmolar solution effects in guinea-pig airways. IV. Lipopolysaccharide-induced alterations in airway reactivity and epithelial bioelectric responses to methacholine and hyperosmolarity. J Pharmacology Exp Ther 308, 37–46.

Jordan, T., 2015. Hydrocarbon Exposures during Tank Gauging and Sampling Operations. www.stepsnetwork.com/member-presentations/file/Tank_GaugingMonitoring_Results%252Epdf.

King, B., Esswein, E., Retzer, K., Snawder, J., Ridl, S., Breitenstein, M., Alexander-Scott, M., Hill, R., 2015. UPDATE: Reports of Worker Fatalities during Manual Tank Gauging and Sampling in the Oil and Gas Extraction Industry. https://blogs.cdc.gov/niosh-science-blog/2015/04/10/flowback-3/.

Krajnak, K., Russ, K.A., McKinney, W., Waugh, S., Zheng, W., Kan, W., Kashon, M.L., Cumpston, J., Fedan, J.S., 2022. Biological effects of inhaled vapors from crude oil. V. Cardiovascular effects. Toxicol. Appl. Pharmacol. 447, 116071. https://doi.org/10.1016/j.taap.2022.116071 (one of seven tandem papers submitted to TAAP).

National Institute for Occupational Safety and Health/Occupational Safety and Health Administration, 2015. Health and Safety Risks for Workers Involved in Manual Tank Gauging and Sampling at Oil and Gas Extraction Sites. https://www.osha.gov/Publications/OSHA3843.pdf.

Retzer, K., Ridl, S., Hill, R., 2015. Oil and gas extraction worker fatalities. In: 2014 Mid-year report: January 1, 2-014 - June 30, 2014. www.cdc.gov/niosh/docs/2015-239/pdfs/2015-239.pdf.

Retzer, K., Schmick, E., Ramirez-Cardenas, A., King, B., Snawder, J., 2018. Gases and Vapors Continue to Pose Hazards on Oil and Gas Well Sites during Gauging, Fluid Transfer, and Disposal. https://blogs.cdc.gov/niosh-science-blog/2018/08/24/oil-and-gas-vapors/.

Ritchie, G.D., Still, K.R., Alexander, W.K., Nordholm, A.F., Wilson, C.L., Rossi 3rd, J., Mattie, D.R., 2001. A review of the neurotoxicity risk of selected hydrocarbon fuels. J Toxicol Environ Health B Crit Rev B 4, 223–312.

Rusiecki, J., Alexander, M., Schwartz, E.G., Wang, L., Weems, L., Barrett, J., Christenbury, K., Johndrow, D., Funk, R.H., Engel, L.S., 2018. The deepwater horizon oil spill coast guard cohort study. Occup. Environ. Med. 75, 165–175.

Sager, T.M., Joseph, P., Umbright, C.M., Hubbs, A.F., Barger, M., Kashon, M.L., Fedan, J.S., Roberts, J.R., 2022. Biological Effects of Inhaled Crude Oil Vapor. III. Pulmonary Inflammation, Cytotoxicity, and Gene Expression Profile (one of seven tandem papers submitted to TAAP).

Selgrade, M.K., Hatch, G.E., Grose, E.C., Illing, J.W., Stead, A.G., Miller, F.J., Graham, J.A., Stevens, M.A., Hardisty, J.F., 1987. Pulmonary effects due to short-term exposure to oil fog. J. Toxicol. Environ. Health 21 (1–2), 173–185. https://doi.org/10.1080/15287398709531010.

Selgrade, M.K., Hatch, G.E., Grose, E.C., Stead, A.G., Miller, F.J., Graham, J.A., Stevens, M.A., Hardisty, J.F., 1990. Pulmonary effects due to subchronic exposure to oil fog. Toxicol. Ind Health 6 (1), 123–143. https://doi.org/10.1177/074823379000600108.

Snawder, J., Esswein, E., King, B., Breitenstein, M., Alexander-Scott, M., Retzer, K., Keifer, M., Hill, R., 2014. Reports of Worker Fatalities during Flowback Operations. https://blogs.cdc.gov/niosh-science-blog/2014/05/19/flowback/.

Sriram, K., Lin, G.X., Jefferson, A.M., McKinney, W., Jackson, M.C., Cumpston, J.L., Cumpston, J.B., Leonard, H.D., Kashon, M.L., Fedan, J.S., 2022. Biological effects of inhaled crude oil vapor. V. Altered biogenic amine neurotransmitters and neural protein expression. Toxicol. Appl. Pharmacol. 449, 116137. https://doi.org/10.1016/j.taap.2022.116137.

Walter, McKinney, Jackson, Mark C., Law, Brandon, Fedan, Jeffrey S., 2022. Automated crude oil vapor inhalation exposure system. Toxicol. Appl. Pharmacol. (One of seven tandem papers submitted to TAAP).

Weatherly, L.M., Shane, H.L., Baur, R., Lukomska, E., Roberts, J.R., Fedan, J.S., Anderson, S.E., 2022. Biological effects of inhaled crude oil vapor. VI. Immunotoxicity. Toxicol. Appl. Pharmacol. 449, 116100 (One of seven tandem papers submitted to TAAP).